Solid State Ionics 230 (2013) 12–15

Contents lists available at SciVerse ScienceDirect

Solid State Ionics

journal homepage: www.elsevier.com/locate/ssi

Degradation of the interfacial conductivity in $LaAlO_3/SrTiO_3$ heterostructures during storage at controlled environments

F. Trier *, D.V. Christensen, Y.Z. Chen, A. Smith, M.I. Andersen, N. Pryds

Department of Energy Conversion and Storage, Technical University of Denmark, Risø Campus, 4000 Roskilde, Denmark

ARTICLE INFO

Article history:
Received 27 April 2012
Received in revised form 27 July 2012
Accepted 2 August 2012
Available online 7 September 2012

Keywords:
Complex oxides
Heterointerfaces
Two-dimensional electron gas
Conductivity stability
Oxygen vacancies
$LaAlO_3/SrTiO_3$

ABSTRACT

The remarkable discovery of a two-dimensional electron gas confined at the interface of the two oxide band-insulators $SrTiO_3$ (STO) and $LaAlO_3$ (LAO) has spurred a great interest in the heterostructure leading to the discovery of a plethora of other exciting properties. Recently, the formation of the interfacial electron gas has also been shown possible when LAO is deposited on STO at room temperature, which leads to the growth of amorphous LAO (a-LAO). Here, we study the development of the interfacial conductivity of LAO/STO heterostructures with crystalline and amorphous LAO top layers in different controlled environments over time. The interfacial conductivity is found to degrade with a strong dependence on the thickness, the crystallinity of the deposited layer and the storage environment. A mechanism for the degradation is proposed and is further utilized to significantly reduce the rate of degradation.

1. Introduction

The development in substrate preparation and film deposition methods within the last 20 years has enabled the production of oxide heterostructures with a quality reaching the level obtainable with current, traditional semiconductor technology [1,2]. The rapid development has enabled the use of oxide heterostructures for reliable applications and rendered these heterostructures the subject of intense research. In particular, the oxide heterostructure composed of $LaAlO_3$ (LAO) deposited on top of $SrTiO_3$ (STO) has recently been the pivot of a tremendous interest [3–5]. In the time span of less than a decade, the heterostructure has been shown to exhibit a plethora of exceptional properties including the formation of a correlated two-dimensional electron gas (2-DEG) [6] with co-existing magnetic [7], superconducting [8] and thermoelectric properties [9] leading to a great potential for device applications [3]. The underlying mechanism for the interfacial conductivity remains, however, disputable despite 8 years of intense studies.

Recently, the formation of 2-DEG has been realized when depositing LAO on STO at room temperature leading to a heterostructure with an amorphous deposited layer of LAO (a-LAO/STO) [10]. The amorphous/crystalline heterostructure shows many similarities to its all-crystalline counterpart (c-LAO/STO) while benefiting from being simpler to both understand and produce. Especially, whereas for the c-LAO/STO heterostructure it has been extensively debated whether the conducting interface arises from an electronic reconstruction at the polar/nonpolar interface [11], cation intermixing [12] or the presence of oxygen vacancies [13], strong indications suggest that only oxygen vacancies can explain the formation of the interfacial conductivity in the a-LAO/STO heterostructure [10]. Studying the similarities and dissimilarities between samples with amorphous and crystalline deposited layers therefore provides a previously unexplored way of understanding the formation of the electron gas in samples with crystalline LAO top films. In particular, comparing the stability of the interfacial conductivity of the two heterostructures provides an important knowledge: The electronic reconstruction is a stable phase and cations are generally frozen at room temperature whereas the lower activation barrier of oxygen diffusion in LAO and STO [14,15] possibly gives rise to a slight mobility of oxygen vacancies. Furthermore, understanding the stability of device performance is vital from an application point of view.

Here, we study the stability of the interfacial conductivity of crystalline and amorphous LAO/STO heterostructures in different controlled environments over time and propose a mechanism for the degradation of the interfacial conductivity.

2. Methods

The a-LAO/STO and c-LAO/STO samples were grown using pulsed laser deposition at room temperature (RT) and 700 °C on TiO_2-terminated STO single crystals in an O_2 pressure of $5\cdot10^{-6}$ mbar and $1\cdot10^{-4}$ mbar, respectively. Note that a higher oxygen pressure was used for the growth of c-LAO at high temperature to prevent bulk conductivity of STO [13]. After deposition, the sample was cooled down to room temperature under the deposition oxygen pressure. It should be noted that for the film deposition at 700 °C, the interface

---

* Corresponding author. Tel.: +45 4677 5614; fax: +45 4677 5858.
E-mail address: fetri@risoe.dtu.dk (F. Trier).

0167-2738/$ – see front matter © 2012 Elsevier B.V. All rights reserved.
http://dx.doi.org/10.1016/j.ssi.2012.08.005

turns insulating if the oxygen pressure is increased to 2 mbar just after film deposition. The deposition was performed using a KrF excimer laser (λ = 248 nm) with a repetition rate of 1 Hz at a fluence of 2.0 J cm^{-2}. The thickness of the c-LAO film was determined using intensity oscillations of the Reflection High-Energy Electron Diffraction (RHEED), whereas the a-LAO thickness was determined using Atomic Force Microscopy (AFM) as the lack of crystallinity disables the use of RHEED.

The interface was electrically contacted using ultrasonically bonded aluminium leads in a Van der Pauw geometry, and the electrical transport properties (sheet resistance, carrier density, mobility) between 10 and 300 K were probed for every sample roughly each week over a duration of 60 days. Between each measurement, the samples were stored in a slight vacuum of 0.8 bar or a pure N_2 or O_2 environment at 1.05 bar.

3. Results and discussion

Depositing amorphous LAO on STO at RT results in the formation of a 2-DEG at the heterointerface displaying a metallic character and transport properties very similar to c-LAO/STO heterostructures (see Fig. 1). This indicates a similar transport mode and origin of charge carriers for the amorphous and crystalline systems. Furthermore, an insulator-to-metal transition is previously demonstrated to exist in the a-LAO/STO heterostructures when the thickness of the a-LAO layer exceeds approximately 1.5 nm [10], closely resembling the transition for the c-LAO/STO heterostructures with a threshold of 4 u.c. (1.6 nm) [16].

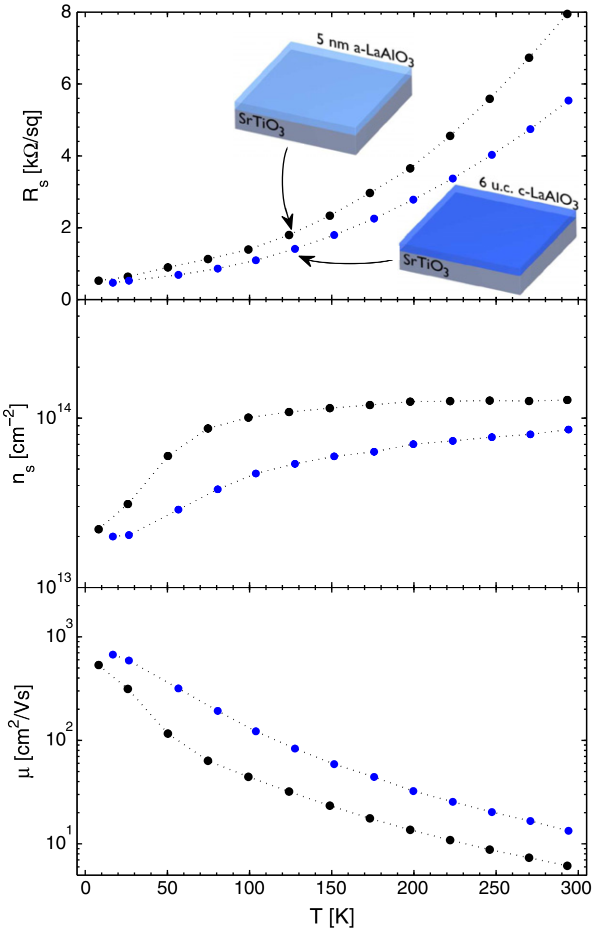

Fig. 1. The transport properties of both amorphous and crystalline LAO deposited on STO display metal-like characteristics. Top pane: the sheet resistance (R_s) decreases gradually with decreasing temperature (T), indicating metallic behavior. Middle pane: the carrier mobility (μ) increases when lowering the temperature. This trend is consistent with phonon scattering as the main cause for a reduced mean free path at high temperatures. Bottom pane: the carrier density (n_s) decreases slowly with decreasing temperature, which is likely to be caused by a subtle lattice distortion in STO below 110 K [25].

Storage of a-LAO/STO heterostructures in a slight vacuum of 0.8 bar for 60 days months leads to a significant increase in the sheet resistance (see Fig. 2) evidencing an relative unstable conducting phase at the interface. The degradation of the interface conductivity is supportive of oxygen vacancies in STO being the origin of the conductivity in the a-LAO/STO heterostructures. The ionic character of STO results in oxygen located in STO being negatively charged, and upon creation of oxygen vacancies, the excess charge of oxygen is donated to the 3*d* states of Ti leading to conductivity. Oxygen vacancies in STO are formed during the deposition of LAO, however, thermodynamically unfavourable - but only modestly mobile - refilling of oxygen vacancies results in the gradual degradation of the conductivity. The observed degradation is consistent with that the conductivity for the heterointerface between $CaHfO_3$ and $SrTiO_3$ has previously been hinted not to be stable at room temperature and ambient atmosphere [17].

Generally, for a modest degradation the increase in the sheet resistance is linear with the rate of degradation being critically dependent on the thickness and crystallinity of the deposited layer and the environment, which the heterostructures are subjected to.

As shown in Fig. 3, the rate of resistance increase is reduced almost 2 orders of magnitude from 2317 (Ω/sq)/day to 60.4 (Ω/sq)/day upon increasing the thickness of the amorphous thin film from 1.5 nm to 5 nm. Similarly, for c-LAO/STO the conductivity becomes roughly 30 times more stable (from 29.3 (Ω/sq)/day to 1.2 (Ω/sq)/day) by adding two extra unit cells of c-LAO to the heterostructure with 4 u.c. c-LAO. This indicates that for thin films, the majority of oxygen diffuses through the LAO layer rather than along the interface or through the STO substrate.

Similarly, albeit a clear conductivity decay is observed for all-crystalline heterostructures (e.g. of 29.3 (Ω/sq)/day for 4 u.c. c-LAO/STO), the degradation is slowed by several orders of magnitude compared to a-LAO/STO of similar top layer thickness. This observation suggests that the diffusion barrier of oxygen migration through the amorphous LAO top layer is smaller than that of the crystalline film leading to the enhanced conductivity degradation in samples with an amorphous top layer. A similar behavior of material morphology on oxygen diffusivity is observed for other oxides such as Al_2O_3 [18,19].

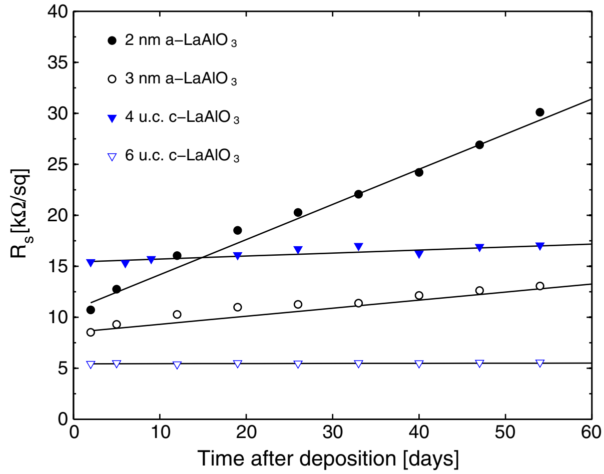

Fig. 2. During storage for 60 days at a pressure of 0.8 bar, samples with an amorphous or a crystalline top layer display an increase in sheet resistance (R_s) at 300 K, which is highly dependent on the thickness and crystalline state of the top layer. The lines represent linear fits of the data points which are used to extract the rate of resistance increase (shown in Fig. 3).